Journal Pre-proof

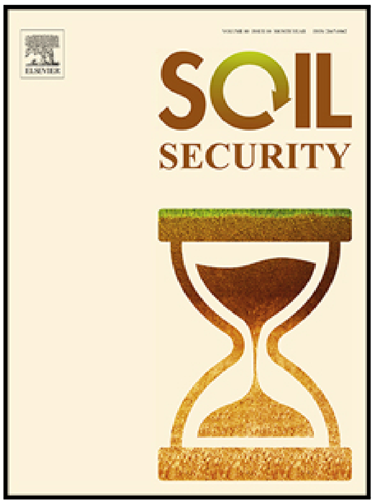

Gas Diffusivity in Peat Soils Across Denmark is Controlled by Soil-Water Characteristics and Effective Porosity

Lene Werner Kristensen , Charles Pesch , Peter Lystbæk Weber ,
Deividas Mikstas , Janni Mosekær Nielsen ,
Anne-Cathrine Storgaard Danielsen , Emmanuel Arthur ,
Mogens Humlekrog Greve , Trine Nørgaard , David A. Robinson ,
Lis Wollesen de Jonge , Per Møldrup

PII: S2667-0062(26)00026-2
DOI: https://doi.org/10.1016/j.soisec.2026.100249
Reference: SOISEC 100249

To appear in: *Soil Security*

Received date: 18 December 2025
Revised date: 28 August 2026
Accepted date: 31 August 2026

Please cite this article as: Lene Werner Kristensen , Charles Pesch , Peter Lystbæk Weber , Deividas Mikstas , Janni Mosekær Nielsen , Anne-Cathrine Storgaard Danielsen , Emmanuel Arthur , Mogens Humlekrog Greve , Trine Nørgaard , David A. Robinson , Lis Wollesen de Jonge , Per Møldrup , Gas Diffusivity in Peat Soils Across Denmark is Controlled by Soil-Water Characteristics and Effective Porosity, *Soil Security* (2026), doi: https://doi.org/10.1016/j.soisec.2026.100249

Highlights (*5, each max. 85 characters*)

- Gas diffusivity (D_p/D_0) was measured on intact peat soil samples across Denmark
- At each matric potential (pF), D_p/D_0 increased linearly with air-filled porosity
- The slope of D_p/D_0 vs. ε (pore connectivity, P) was excellently correlated with pF
- Effective porosity (ε at pF 3) and P were used to create a predictive D_p/D_0 model
- The predictive D_p/D_0 model was successfully validated against independent data

Gas Diffusivity in Peat Soils Across Denmark is Controlled by Soil-Water Characteristics and Effective Porosity

Lene Werner Kristensen[a], Charles Pesch[b], Peter Lystbæk Weber[b], Deividas Mikstas [b] Janni Mosekær Nielsen[a], Anne-Cathrine Storgaard Danielsen [b], Emmanuel Arthur [b], Mogens Humlekrog Greve [b], Trine Nørgaard [b], David A. Robinson[c], Lis Wollesen de Jonge[b], Per Møldrup[a]

[a] *Division of Civil and Environmental Engineering, Department of the Built Environment, Aalborg University, Thomas Manns Vej 23, Aalborg, DK 9220, Denmark*

[b] *Section of Soil Physics and Hydropedology, Department of Agroecology, Aarhus University, Blichers Allé 20, 8830 Tjele, Denmark*

[c] *UK Centre for Ecology and Hydrology, Environment Centre Wales, Bangor, United Kingdom*

Keywords: Gas diffusion coefficient, gas diffusivity, peat soils, soil-water potential, effective porosity, aeration limit, pore-network tortuosity

Abstract

The soil-gas diffusivity (ratio of gas diffusion coefficients in soil and pure air), D_p/D_0, controls the mobility of gases in variably saturated soils, including aeration, emission and uptake of greenhouse gases. Previous soil-gas diffusivity studies have focused on lower-organic soils. Here, D_p/D_0 was measured on intact soil cores at six different soil-water matric potentials between -30 and -1000 cm H_2O (pF between 1.5 to 3) on 127 Danish peat top soils (12-52% SOC). The SOC level was not found to be main control of D_p/D_0 for peat soils. D_p/D_0 versus soil-air content (ε) curves varied as much within a narrow SOC interval (e.g., 30-36% SOC) as for the whole range. In contrast to previous observations for lower-organic soils, it was found that at each pF level, D_p/D_0 increased linearly with ε, the slope, the Penman pore continuity index P, increased linearly with pF. Previous D_p/D_0 models developed for lower-organic soils (typically < 4% SOC) failed to describe D_p/D_0 for peat soils. A soil-water characteristic curve-dependent model (Buckingham-Burdine-Campbell, BBC) well predicted D_p/D_0 for peat soils. A modified WLR model with inputs of actual and effective air-filled porosity (ε*, taken as ε around pF3) was developed. The BBC and modified WLR models were successfully validated against independent data for high-organic soils representing different climate zones and organic matter quality. This work provides a better understanding of and models for gas diffusion in high-organic soils, setting a platform for including soil-air phase properties when evaluating soil functions, security, and capital.

1 Introduction

Soil provides a large number of ecosystem services ranging from food production to climate mitigation (Adhikari and Hartemink, 2016; Chirol et al., 2025). The main soil ecosystem service has been food production which has also been one of the main topics of soil research (Pozza and Field, 2020). Soil and food security are linked as 95% of the global food supply is estimated to depend on sustainable soil management practices (Pozza and Field, 2020).

As the impacts of climate change become increasingly evident, the recognition of the soil's role in climate mitigation has likewise increased. Soil organic carbon (SOC) represents the largest terrestrial carbon pool. Peatland soils play a significant part in the global carbon cycle, as they account for one-fifth of the total global SOC (Friedlingstein et al., 2022; Leifeld et al., 2019). This leaves the potential for a large amount of SOC being emitted from peat soils as carbon dioxide (Leifeld et al., 2019). Methane is the second most important greenhouse gas (GHG) after carbon dioxide (Saunois et al., 2020). It is estimated that approximately 30% of all global methane emissions can be attributed to peat and wetland areas (Kirschke et al., 2013). The emissions of GHG from peat soils are closely related to transport, or the lack thereof, in the soil pore space, as many of the gas-forming processes are governed by the availability of oxygen (Bridgham et al., 2013).

Soil gas diffusion plays a crucial role in transporting greenhouse gases such as methane through the soil (Kruse et al., 1996) and in the transport of oxygen to enable the growth of plant roots and bacterial communities (Rolston and Moldrup, 2002). Gas diffusion has long been considered the primary transport mechanism in the soil-air phase (Moldrup et al., 2013; Rolston and Moldrup, 2012). The soil gas diffusion is typically described by the normalized gas diffusivity (D_p/D_0), which describes the ratio between the gas diffusion coefficient in the soil and the gas diffusion coefficient in free air for the specific gas. The gas diffusivity is normalized so it is applicable for all gases.

Gas diffusion is governed by the tortuosity and connectivity of the air-filled pore-space (Chamindu, T. K. K. et al., 2011; Moldrup et al., 2013). Models for gas diffusivity in soils have mainly been developed for (Chamindu, T. K. K. et al., 2011; Moldrup et al., 2013)mineral-dominated agricultural soils; however, newer studies suggest that these models are not able to accurately describe the gas diffusivity of different habitat types (Kiuru et al., 2022; Maier and

Lang, 2019). Traditional models did not accurately describe the gas diffusivity in high organic Finnish peat soils (Kiuru et al., 2022) and the study by Maier and Lang (2019) on forest soils suggests that traditional models do not capture the diversity found in habitats dominated by plant material in different stages of degradation. The two studies suggest that the effects of SOC in high organic soils call for different modelling approaches, and it seems that traditional models are not scalable to include high organic soils.

Likewise, others have found that there exists a threshold for which a soil (mixture of components) behaves like the pure form of its major constituent, e.g. Zhu et al. (2019) and Yin et al. (2021). Hence, increasing the concentration of the constituent in question beyond that threshold does not necessarily alter the soil function in question, however, that is to be further explored. The influence of SOC and habitat type are relevant factors to include when considering which gas diffusivity models should be used, as traditional models did not show a satisfying prediction ability. This suggests that simply using a "one size fits all" approach will not provide a good basis for soil gas diffusivity.

1.1 Objectives

We hypothesize that high organic soils will have different D_p/D_0 controls and behavior compared to more mineral soils. The hypothesis was tested through four main objectives:

(1) Present soil-gas diffusivity (D_p/D_0) measurements at different suction levels (pF) on intact soil cores from peat top soils across Denmark.
(2) Investigate the main physical controls of D_p/D_0 in peat soils.
(3) Evaluate if present D_p/D_0 models typically developed for lower-organic soils are realistic and accurate for peat soils and develop a simple, accurate model for high-organic soils.
(4) Preliminary validate the new gas diffusivity model against independent data and discuss the importance of including soil air phase properties when evaluating soil functions, security, and capital.

2 Materials and Methods

2.1 Soils

This study includes soil samples collected across a total of 127 lowland and peatland agricultural areas in Denmark from 2021-2023, Figure 1. For the purpose of testing the hypothesis, only high organic soils with SOC > 12% were included in this study. In this study, high organic soils are defined as SOC > 12%, while low organic mineral soils are defined as SOC < 12%. At each site, 3-4 undisturbed soil cores (100 cm^3, 6.1 cm inner diameter, 3.4 cm height) were collected at 0-20 cm depth together with a bulk soil sample. Prior to sample collection, vegetation and litter were removed from an area of approximately 1 m^2, and all samples were collected within this area as described in Danielsen et al. (2025).

The soil cores were stored at 2°C between collection and further analysis.

2.2 Measurements

2.2.1 Bulk soil

Before the measurements were carried out, the bulk soil samples were air-dried, crushed, and sieved to <2 mm. Total carbon (TC) was measured by dry combustion using a Vario MAX cube (Elementar Analysensysteme AG). In the presence of carbonates these were corrected for to obtain SOC.

Particle density was determined by the water displacement method as described by (Flint and Flint, 2002).

2.2.2 Undisturbed soil cores

The intact soil cores were saturated from below in a tension table and subsequently drained to soil-water matric potentials of -30, -50, and -100 cm H_2O; for more negative matric potentials (-300, -500, and -1000 cm H_2O), a Richards pressure plate apparatus was used.

At each drainage step, the gas diffusion coefficient of the intact soil cores was measured using oxygen as the tracer gas. The measurements followed the one-chamber, steady-state method (Rolston and Moldrup, 2002), using the device as presented in Schjønning et al. (2013). The relative diffusivity was obtained by dividing the oxygen diffusion coefficient of the soil (D_p) by the oxygen diffusion coefficient in free air (D_0, set to 0.205 $cm^2\ s^{-1}$ following Schjønning et al. (2013)).

After the last measurement at -1000 cm H_2O, the dry bilk density (ρb, g/cm^3) of the soil cores were determined after oven-drying them at 105 °C for 24 hours.

The total porosity of the soil cores (Φ, $cm^3\ cm^{-3}$) was calculated from the measured particle density and bulk densities.

2.2.3 Soil water characteristics

The Campbell (1974) water retention model was used to describe the soil water characteristics of the peat soils. The model (Eq. [1]) was fitted to the measured soil water retention data between pF 1.5 and 3.

	$\Psi = \Psi_e \left(\frac{\theta}{\theta_s}\right)^{-b}$	[1]

where Ψ_e is the air entry potential (in cm H_2O), Θ_s is the water content at saturation (in $cm^3\ cm^{-3}$) and set equal to Φ; b can be interpreted as the soil pore-size distribution index (Moldrup et al., 2001). Both Ψ_e and b are fitting parameters.

An overview of the measured and calculated soil characteristics is shown in Table 1, where the average value for each SOC interval is shown as well as an overall average for the entire dataset. The dataset represents a large variation for all the characteristics considered in this study.

2.3 Gas diffusivity models

In this study we compare the measured gas diffusivities against commonly used models for gas diffusivity. The models vary in complexity and input parameters from the simplest ε-based models ((Buckingham, 1904; Penman, 1940)) to the most complex model (Buckingham-Burdine-Campbell by Moldrup et al. (1999)) which requires knowledge of the entire water retention curve.

Buckingham (1904) suggested,

$$\frac{D_p}{D_0} = P\ \varepsilon^X \quad [2]$$

where ε is air-filled porosity, also called soil air content (cm^3 soil air/cm^3 soil), and P and X are fitting constants. Buckingham (1904) recommended P = 1 and X = 2 based on a few measurements. The measured relative diffusivities were fitted to the Buckingham (1904) diffusivity model (Eq. [2]) to infer the tortuosity of the pore space by the fitting parameters P and X assumed as 1. Numerous versions of Eq. [2] have later been proposed, including P = 1 and X = 2.5 considered by both Ball (1981) and Currie (1960), which Weber et al. (2020) also suggested for organic, Greenlandic soils.

Penman (1940) suggested a variable P and the simplified version of the Buckingham model

	$$\frac{D_p}{D_0} = P\varepsilon$$	[3]

Penman (1940) furthermore set P = 0.66 (corresponding to Eq. [2] with P = 0.66 and X = 1). Most studies (e.g. Chamindu et al. (2015); Petersen et al. (1994)) have found the Penman model to overestimate D_p/D_0 for variably saturated soils but found it highly accurate for dry (void of water) soil conditions. Previous studies, such as Rust et al. (1957) and Anderson et al. (2000), have suggested alternative Penman P-values with some success, and as such, in the present study on intact peatland soils, we will consider Penman P as a fitting parameter.

Millington and Quirk (1961) suggested the addition of total porosity (Φ).

	$$\frac{D_p}{D_0} = \frac{\varepsilon^{\frac{10}{3}}}{\Phi^2}$$	[4]

Millington and Quirk (1961) have been tested for peat soils by Kiuru et al. (2022) who found that the model relatively accurately described D_p/D_0 in top soils but not in sub soils.

Moldrup et al. (2000a) used the Penman (1940) model [Eq.3] as a platform (as a reference-point model at dry conditions) to develop the so-called Water-induced Linear Reduction model (WLR-Penman),

	$$\frac{D_p}{D_0} = P\varepsilon^X \frac{\varepsilon}{\Phi}$$	[5]

They used the combination of the WLR concept and the Penman gas diffusivity model (for dry soils) and thereby suggested P=0.66 and X=1. This combination of parameters was found to perform accurately by Moldrup et al. (2000a) for sieved, repacked soils.

Moldrup et al. (2000b) proposed the Macro Porosity Dependent (MPD) model.

	$\frac{D_p}{D_0} = 2\varepsilon^3 + 0.04\varepsilon$	[6]

They found this model accurately described (R^2=0.97) the relationship between D_p/D_0 and air-filled porosity for a wide range of mineral soils at pF 2. Kiuru et al. (2022) found that the model relatively accurately described D_p/D_0 at pF 2 for peat in both top soils and sub soils.

Chamindu et al. (2011) developed the today frequently used Generalized Density Corrected (GDC) model for predicting gas diffusivity in undisturbed, variably saturated soils, from the previous Density Corrected (DC) and SWC-dependent D_p model by Chamindu et al. (2011) and Moldrup et al. (2000b). The GDC model also includes both air-filled porosity and total porosity (Φ) in the prediction of D_p/D_0.

	$\frac{D_p}{D_0} = 0.5\Phi \frac{\varepsilon}{\Phi}^{2+1.38\Phi}$	[7]

Like Moldrup et al. (2000b), this study also considered D_p/D_0 behavior at individual pF values.

Moldrup et al. (1999) combined the Buckingham expression with the Campbell pore size distribution model and the Burdine capillary tube model to develop the Buckingham-Burdine-Campbell (BBC) model.

	$\frac{D_p}{D_0} = \Phi^2 \frac{\varepsilon}{\Phi}^{2+3b}$	[8]

In this model, the pore-size distribution is accounted for by incorporating the Campbell *b* parameter.

This study further expands the WLR-Penman model by introducing the air-filled porosity at pF 3 (- 1000 cm H2O) instead of the total porosity, leading to Eq. [9].

	$$\frac{D_p}{D_0} = P\varepsilon\ \frac{\varepsilon}{\varepsilon^*}$$	[9]

where ε* serves as an anchor point following Pittaki-Chrysodonta et al. (2018) for the Campbell water retention function.

2.4 Statistical methods

To compare the model performance, three statistical measures were chosen: Root Mean Squared Error (RMSE), Nash-Sutcliffe model efficiency (NSE), and Akaike's Information Criterion (AIC). These statistical measures were chosen based on their ability to complement each other and accurately describe the different gas diffusivity models used in this study.

The RMSE provides an average prediction uncertainty of the model in question and can be used as a measure of accuracy (Hyndman and Koehler, 2006).

	$$RMSE = \sqrt{\frac{1}{n}\sum_{i=1}^{n}(M_i - O_i)^2}$$	[10]

where *M* is the model prediction, *O* is the observed measurement, and *n* is the number of observations. The RMSE is scale-dependent and, as such, does not allow for comparison between different datasets. In this study, the RMSE is used to compare different models applied to the same dataset.

In contrast to the RMSE, the NSE performance measure is an absolute value of model performance (Nash and Sutcliffe, 1970).

$$NSE = 1 - \frac{\sum_{i=1}^{n}(M_i - O_i)^2}{\sum_{i=1}^{n}(O_i - \bar{O})^2} \quad [11]$$

where M is the model prediction, O is the observed measurement, and n is the number of observations. The NSE punishes systematic model bias, as it evaluates the model performance against the bisector line (Nash and Sutcliffe, 1970). As the NSE gives an absolute value of model performance, it can be evaluated across datasets, with NSE=1 being a perfect match, NSE=0 means that the model predictions are as accurate as the mean of observations, and NSE<0 means that using the mean of observations will provide a better predictor than the evaluated model (Nash and Sutcliffe, 1970).

However, as neither of the previous performance measures takes model complexity into account, the AIC is included as a performance metric. The AIC incorporates the number of model parameters, recognizing that more complex models with additional parameters often yield a better fit due to overfitting from an increased number of degrees of model freedom. Because the models tested in this study differ in their number of model parameters, considering model complexity by the AIC is essential for identifying the best model.

$$AIC = n\left\{\ln(2\pi) + \ln\left[\frac{\sum_{i=1}^{n}(M_i - O_i)}{n-k}\right] + 1\right\} + \mathrm{k} \quad [12]$$

where M is the model prediction, O is the observed measurement, k is the number of model parameters, and n is the number of observations.

Variations of this combination of performance measures have previously been used in studies within the soil-porosity phase, such as Moldrup et al. (2004) and Nielsen et al. (2018).

3 Results and discussion

The dataset in this study is unique because of the large variations in soil organic carbon content, bulk density, particle density, and air-filled porosity at pF 3. The bulk density of the samples varied between 0.09 and 1.19 g/cm^3, directly influencing the total porosities (from 0.51 to 0.95 cm^3/cm^3). Particle density was seen to decrease with increasing SOC content (Ruehlmann, 2020).

3.1 SOC-dependence of soil-air properties

Previous studies on mineral soils, e.g. Moldrup et al. (2013), have suggested that the basic soil-water and soil-air properties of a soil should be influenced by the SOC content. As shown in Figure 2, this is not as clear for the peatland soils in this study. Figure 2 (A) shows retention curves for three selected samples from different locations, all with SOC ~ 35 %, and Figure 2 (B) shows the linearized soil-water retention curve for the same three samples fitted to the Campbell (1974) soil-water retention model. Despite the three samples having similar SOC contents at around 35% (34.63%, 35.03% and 35.62%), the samples show very different water retention characteristics and thus different Campbell b values (4.61, 7.49 and 28.03). The difference between the three soils is to be found in the porosities and bulk density, as these vary noticeably between the three samples (BD =0.18-0.45 g/cm^3, ε*= 0.134-0.690 cm^3/cm^3). Similar SOC contents can exist in widely different soil structures and as thus widely different transport properties. This indicates that a more descriptive parameter is needed. Examining the relationship between the ε* and the Campbell b values, Figure 2(C) also shows that the retention parameter (Campbell b) seems linearly dependent on the inverse of ε*.

The absence of a SOC-dependent pattern is also evident in Figure 3(A). Although gas diffusivity is plotted against soil-air content and grouped by SOC, no consistent trend appears, suggesting that SOC has little influence on D_p/D_0 in this dataset. In contrast, when the dataset is grouped by moisture conditions (matric potential; Figure 3 (B)), distinct patterns emerge, indicating that moisture has a stronger influence on D_p/D_0 than SOC.

3.2 SOC-dependence in Buckingham tortuosity-connectivity parameter

The dataset in Figure 3(A–B) can be framed/bounded by Buckingham tortuosity–connectivity parameter X (Eq. [3], using P=1). Buckingham X ranges from 1.5 to 6 which indicates substantial variation in tortuosity, connectivity, and constrictions in the pore network of the samples in this study. Marshall (1959) suggested X=1.5 for mineral soils, which is also the lower boundary for all D_p/D_0 measurements in this study. Furthermore, Moldrup et al. (2013) found X=1.5 to well describe gas diffusivity in relatively structureless soils, which suggests a higher degree of complexity in the pore network of the peat soils compared to mineral soils.

The best fit for the complete dataset in this study was X = 2.53 (RMSE = 0.027), which was close to the X value found by Weber et al. (2020) (X = 2.5) for Greenlandic soils (SOC=0.16-10.5%), indicating some similarities in terms of pore-network tortuosity and connectivity between the Danish and Greenlandic soils. This suggests that the high SOC shares some similarity between Danish peat and the highly sandy Greenlandic soils, as both are likely saturated with SOC (Dexter et al., 2008). Looking at single samples with comparable SOC (around 35 % SOC) introduced in Figure 2 (A-B), it is clear that the SOC content does not determine the gas diffusivity for the same three samples in Figure 3 (C). The three samples display almost as wide a range of Buckingham X-values as the entire dataset when Buckingham X is fitted to the samples individually.

Comparing the relationship between the gas diffusivity and the soil-air content for the peat soils to the threshold value for reaeration set by Schjønning et al. (2007) (D_p/D_0 =0.02), it also becomes clear that there is no influence of SOC in Figure 3 (A). Both soils from the highest interval (>36% SOC) and the lowest interval (12-30% SOC) are found below the aeration limit.

3.3 Gas diffusivity dependence of soil-air content

Figure 4 shows D_p/D_0 versus ε for the peat soils at 6 different matric potentials, confirming lower transport, higher tortuosity, and more linear behavior than for mineral soils. This becomes apparent when comparing the data to the non-linear Buckingham model ($D_p/D_0 = \varepsilon^2$), which is often found to be suitable for dry mineral soils (Currie, 1960; Moldrup et al., 1999). Both the best fit for the Penman pore continuity index (P) and the linearity is found to increase (higher R^2) with matric potential (pF). This suggests that the peat soils have a different D_p/D_0 behavior than seen in mineral soils, which is previously shown to follow the exponential Buckingham (1904) model and behave less linearly with ε as they dry (Currie, 1960; Moldrup et al., 1999).

The strongest linearity between gas diffusivity and the soil-air content and the highest value of Penman P are seen at pF 3, where the Penman P is fitted at 0.25, which is notably lower than previous mineral-based studies such as Anderson et al. (2000), suggesting P=0.5, and the original Penman (1940) model, suggesting P=0.66. The peat soils are presumed to be well drained at pF 3, as pores greater than 30 micrometres have drained; thus, it is presumed that the gas diffusivity is mostly limited by soil structure and can be compared to similar studies on dry mineral soils (Schjønning, 1992).

The progression through Figure 4 also shows that the peat soils need a higher suction level for the pores to be open for gas transport. Field capacity is typically seen at around or below pF 2 for mineral soil (depending on area), whereas the peat soils are still mostly beneath the limit for adequate aeration (D_p/D_0 =0.02, (Schjønning et al., 2007)) at pF 2 and are only mostly open at pF 2.5. This is vital to understanding the role of peat soils from both a climate and food production perspective. Peat soils need drier conditions to allow reaeration, limiting the gas exchange. Thereby, the production of climate gases, but also the oxygen for plant roots can be limited in peat soils as a result of the limited gas exchange (Kruse et al., 1996).

The increasing linearity in the D_p/D_0 vs. ε relationship with increasing matric potential is not unique to the Danish peat soils in this study. Compared to Finnish peat soils from Kiuru et al. (2022), the same tendency is observed as seen in Figure 5 (A), where the Penman P is shown as a function of the matric potential for the P-values found in Figure 4 (A-F) and P-values from Kiuru et al. (2022). The best linearity is seen at pF 3; however, as is shown in Figure 5 (B), a satisfying goodness of fit (R^2-value) is reached at pF 2.7. The R^2 values from Figure 4 (A-F) are compared to the suction level (pF), and a decrease in the slope is seen between pF 2.7 and pF 3 compared to the additional pF values. This suggests that a functional Penman P could potentially be even lower than the P=0.25 suggested in this study, and thus even further from the typically proposed P values (Anderson et al., 2000; Penman, 1940; Rust et al., 1957).

3.4 Bimodal pore-network impact

Figure 6 (A-D) compares four gas diffusivity models; the original Penman (1940) [Eq.3], the mineral-soil developed GDC model [Eq. 7], the retention-based BBC model [Eq. 8], and the effective porosity (ε*) dependent WLR model.

Overall, the two models that best described D_p/D_0 data were the pore-size distribution dependent BBC model (Figure 6 (C)) and the new ε* dependent WLR model (Figure 6 (D)), with ε* taken as the air-filled porosity at pF 3 or pF 2.7. The good performance of the ε* dependent model can be explained as follows. For a given ε value below ε*, the volumetric water content situated within the diffusion-relevant porosity simply equals ε*-ε. This volumetric water content will, for a given ε value, increase with ε*. Due to the diffusion coefficient in water being approximately 10,000 times lower than in free air, even small water bridges at the bottle necks can effectively block the gas diffusion (Moldrup et al., 2007). Hereby, higher ε* should markedly reduce soil-gas diffusivity at any given ε value, as expressed by the ε/ε* term in the ε*-dependent WLR model. Recent and frequently used D_p/D_0 models, also taking into account such water blockage effects but linking them to total porosity (e.g., the WLR-Penman and GDC models (Figure 6 (B)), failed to capture the measured level of D_p/D_0 and shape of D_p/D_0 versus ε relations in these soils. The high performance of the ε* dependent WLR model for peat soils suggests peat is functionally characterized by a bimodal pore-network system with minimum water blockage of air-filled pore-networks occurring around pF 2.5 - 3 when pores > 3-10 micrometers (macro- and mesopores) are drained. This supports pore-network analyses of peat soils by Hamamoto et al. (2016) and Rezanezhad et al. (2012) also suggesting bi-modal pore-networks.

The shown links and dependencies between D_p/D_0 and the Campbell pore-size distribution index (BBC model) and the air and corresponding gas-phase blocking water contents at pF 3 (ε*-modified WLR model), as well as the observed near-perfect linear relation between the Penman pore connectivity index P and magnitude of soil-water potential (pF) all suggest that the soil-water retention curve and the pore size distribution controls the pore-network connectivity and tortuosity and thus D_p/D_0 in multiple ways (including shape and volume content of certain pore classes).

3.5 Independent model test

Widely different values of Buckingham X for similar SOC contents were observed for the dataset, which leads to believe that not only the SOC content but also the state of degradation is relevant in understanding the complexity of SOC influence. The state of degradation has the ability to change the soil matrix drastically within the same SOC content interval. For traditional peat soils with visible plant structure, a much more heterogeneous soil matrix is seen and as such a potential for a more tortuous pathway. Irregular shapes, platy structures, etc., can lead to very different tortuosity while still exhibiting similar total porosities. This leads to hypothesizing that using ε* as a reference instead of total porosity better reflects the available pore space for gas transport. Therefore, we performed a preliminary independent D_p/D_0 model test for soils with different peat decomposition states, located in different countries and climate zones.

Figure 7 shows the test for six different soils/datasets, applying the GDC model, the BBC model and the new ε* modified WLR model. The six soils/datasets represent different SOC levels, different compaction levels and different degrees of decomposition. Figure 7 (A) and (B) shows mineral and non-peat (<12% SOC) soils from Greenland (Pesch et al., 2021) and Danish lowland soils from the same measuring campaigns as the peat soils used in this study. The three models well describe the gas diffusivity vs ε relation in the Greenlandic mineral soils, whereas the GDC model slightly underpredicts for the non-peat Danish soils. This trend is also seen for the Japanese peat soils in Figure 7 (C) and (D) and for the Thai oil palm field soil in Figure 7 (E) (Iiyama et al., 2012). This suggests that a total porosity-based model does not suffice to describe more organic soils, in agreement with Figure 6 (B). The Japanese sub soils (Figure 7 (D)) and the Finnish mor soils (Figure 7 (F)) (Laurén and Mannerkoski, 2001; Laurén et al., 2000) demonstrate the effect of decomposition on the gas diffusivity. The two soils represent soils with less decomposition and more noticeable plant structures. Despite having similar physical properties to the other soils in Figure 7, the gas diffusivity vs ε relationship is generally lower. The BBC model overpredicts for the two soils, while the GDC model underpredicts for the Japanese sub-soil but relatively well describes the Finnish mor soils despite the soils being well outside the optimal SOC intervals for the GDC model. This may be contributed to a more plate-like structure of the less decomposed soils which creates a more tortuous pathway. Hereby, the pore network might resemble the pore structure of more mineral soils (Currie, 1960; Laurén et al., 2000).

The ε* modified WLR model fits well across all soils despite the soils displaying widely different physical characteristics from the Danish lowland peat soils for which it is developed. The model showed accurate against soils outside the intended SOC content (Figure 7 (A) and (B)), peat soils from different climate zones (Figure 7 (C), (D) and (E)), and a sparsely degraded forest soil (Figure 7 (F)).

Due to very limited available data for gas diffusivity in intact, high organic soils at controlled pF conditions and with knowledge of the soil water characteristics curve, Figure 7 only represents a preliminary model validation of the considered D_p/D_0 models. However, as discussed by Page et al. (2011), global peatlands vary greatly in structure, composition and physical characteristics, and thus, more in-depth validation is recommended when additional data becomes available.

3.6 Further exploration of the peat functional behavior

Both the BBC model and the ε* modified WLR model show a satisfactory prediction ability for peat soils for both the current dataset across Denmark (Figure 6) and for the preliminary validations (Figure 7). This allows for further exploration of the peat functional behavior.

Figure 8 (A) and (B) shows the required air-filled capacity needed to reach reaeration at D_p/D_0 =0.02 and limited aeration at D_p/D_0 =0.005 (Schjønning et al., 2007) as a function of air-filled porosity at pF 3, ε*, in the ε* modified WLR model (A) and the inverse Campbell pore-size distribution index, 1/b, in the BBC model (B). For both models, the required air-filled capacity needed for reaeration exceeds the normally set requirement of ε=0.10 cm^3/cm^3 suggested by da Silva et al. (1994).

The more realistic description of D_p/D_0 as a function of ε for peat soils using soil-water characteristic based D_p/D_0 models allows for more accurately predicting required ε-levels for sufficient soil aeration, of benefit for securing crop productivity and quality. It also allows for more accurately estimating soil greenhouse gas emissions/uptake, where many large-scale (up to global scale) standard simulation tools and studies still in general apply the Penman (1940) or Millington and Quirk (1961) type gas diffusivity models. Both model approaches have shown questionable accuracy for both mineral and high-organic soils (Moldrup et al. (2013); and present study).

Regarding greenhouse gasses Bridgham et al. (2013) and Kruse et al. (1996) have suggested that a precise description of D_p/D_0 is essential to understand the production, emissions and uptake of methane. Kruse et al. (1996) showed that methane uptake (oxidation) in organic forest soil is dependent on oxygen penetration depth within the soil column and thus a well-connected pore-network. Figures 8 (A) and (B) suggest that a much higher aeration threshold than 0.10 cm^3/cm^3 should be considered when estimating air exchange in peat soils. The previous rule of thumb of 0.10 cm^3/cm^3 air-filled pore space is not necessarily enough to ensure adequately connected pore space for gas transport. This is highly relevant for global estimations of greenhouse gas budget, as the carbon stocks and unique retention properties of peat soils make them especially valuable as a climate mitigator (Leifeld et al., 2019).

Figure 8 (C) and (D) link pore-network tortuosity to the air-filled porosity at pF 3 and the inverse Campbell pore-size distribution and show that an increase in air-filled porosity at pF 3 and decrease in Campbell b (increase in inverse Campbell b) gives an increase in pore-network tortuosity. This is caused by a change in moisture conditions (water content in the meso- and macropore space) that causes more water bridging and higher tortuosity. The Campbell pore-size distribution index, b, characterizes pore connectivity and as such all parameters linked to transport mechanisms in the soil-pore-space. A recent study by Mikštas et al. (submitted) found the inverse Campbell pore-size distribution to be the best predicter for weight-based soil basal respiration rate (BRR) which is an important indicator of potential CO_2 production and emission. The study also found a significant relation between 1/b and all scaling of BRR for Danish lowland soils also considered in this study and highlights the importance of pore-size distribution and gas diffusivity when considering transport and fate of greenhouse gasses in peat soils.

This study highlights the need to consider the gas-phase system as fundamental dimension within soil quality and value within the Soul Security Assessment Framework and when quantifying soil capital (Evangelista et al., 2024; Francos et al., 2024). The value of the gas-phase system extends beyond its direct influence on soil aeration; it governs the exchange of gases between soil and atmosphere and supports biological and biogeochemical processes that sustenance ecosystem functioning. Consequently, the condition and resilience of the soil gas-phase system influence the capacity of soils to generate ecosystem services, making it an important contributor to our understanding of soil capital.

4 Conclusions

We presented soil-gas diffusivity (D_p/D_0) measurements on intact peat soil cores at six different suction (pF) levels and representing a very wide interval of SOC content (12-52 %).

From measurements and data analyses, it was concluded that:

- The SOC level was, per se, not a main control of D_p/D_0 in peat soils. This was shown by the variation in D_p/D_0 versus ε relations within a narrow SOC interval (30-36% SOC as an example) was as large as for all 127 peat soils (12-52% SOC) as a whole.
- The pF level (representing the level of drained pore size) was identified as a main driver of D_p/D_0. A quasi-linear but different relation between D_p/D_0 and soil-air content (ε) was found at each pF level, underscoring this conclusion.
- The slope of the D_p/D_0 versus ε relation (Penman pore connectivity index, P) increased linearly with pF. In addition, the derived pore-network tortuosity (T) in peat soils was directly controlled by suction (pF) level, and the relationship was linear over a large part of the pF range.
- Commonly used predictive models describing D_p/D_0 dependency on air-filled and total porosity, such as the GDC model (Chamindu, T. K. K. et al., 2011), failed to predict measured D_p/D_0 for peat soils. This shows the need for the new predictive model presented in this study.
- A Campbell pore-size distribution index (Campbell b) dependent model for D_p/D_0 (Moldrup et al., 1999) well predicted D_p/D_0, further supporting that the soil-water characteristics largely control D_p/D_0 in peat soils.

- The suggested D_p/D_0 model based on only air-filled (ε) and effective (ε*) porosities (the ε* modified WLR model), yielded equally high accuracy for peat soils.
- Preliminary validation of the models against independent data across organic matter contents and degradation states and climate zones confirmed the soil water characteristic dependent models (BBC and ε* modified WLR) performed well and best.

This study showed a fundamentally different behavior of D_p/D_0 and its relation with ε and pF in peat soils compared to more mineral soils. This needs to be recognized when applying predictive D_p/D_0 models, hereunder using these models in the context of strengthening the Soil Security Assessment Framework through a better understanding of the soil-air phase. With the increased knowledge of soil-air phase properties for both mineral and organic soils and the importance of air capacity (ε) and gas diffusivity (D_p/D_0) in controlling soil GHG emissions and mitigation, soil carbon stocks, and soil aeration and productivity, the soil-air phase should have an increased role when evaluating soil security and capital.

Acknowledgments

This work was supported by the Ministry of Food, Agriculture and Fisheries of Denmark (TargWET, 33010-NIFA-22-789) and the European Union Horizon Europe research and innovation program under grant agreement No. 101086179 (AI4SoilHealth). Views and opinions expressed are, however, those of the authors only and do not necessarily reflect those of the European Union or the Research Executive Agency (REA). Neither the European Union nor the granting authority can be held responsible for them.

References

Adhikari, K. and A.E. Hartemink, 2016. Linking soils to ecosystem services — A global review. Geoderma. 262, 101–111. https://doi.org/10.1016/j.geoderma.2015.08.009.

Anderson, A.N., J.W. Crawford and A.B. McBratney, 2000. On Diffusion in Fractal Soil Structures. Soil Sci. Soc. Am. J. 64, 19–24. https://doi.org/10.2136/sssaj2000.64119x.

Ball, B.C. 1981. Pore characteristics of soils from two cultivation experiments as shown by gas diffusivities and permeabilities and air-filled porosities. J. Soil Sci. 32, 483–498. https://doi.org/10.1111/j.1365-2389.1981.tb01724.x.

Bridgham, S.D., H. Cadillo-Quiroz, J.K. Keller and Q. Zhuang, 2013. Methane emissions from wetlands: biogeochemical, microbial, and modeling perspectives from local to global scales. Global Change Biol. 19, 1325–1346. https://doi.org/10.1111/gcb.12131.

Buckingham, E. 1904. Contributions to our knowledge of the aeration of soils. Bulletin no. 25, Bureau of Soils, Government Printing Office, Washington, DC.

Campbell, G.S. 1974. A Simple Method for Determining Unsaturated Conductivity From Moisture Retention Data. Soil Science. 6, 311–314. https://doi.org/10.1097/00010694-197406000-00001.

Chamindu, T.K.K., P. Moldrup, P. Schjønning, K. Kawamoto, T. Komatsu and L.W. de Jonge, 2011. Generalized Density-Corrected Model for Gas Diffusivity in Variably Saturated Soils. Soil Sci. Soc. Am. J. 75, 1315–1329. https://doi.org/10.2136/sssaj2010.0405.

Chamindu, T.K.K.D., P. Moldrup, P. Schjønning, L.W. de Jonge, K. Kawamoto and T. Komatsu, 2011. Density-corrected models for gas diffusivity and air permeability in unsaturated soil. Vadose Zone J. 10, 226–238. https://doi.org/10.2136/vzj2009.0137.

Chamindu, T.K.,K., L.W. de Jonge, K. Kawamoto, T. Komatsu and P. Moldrup, 2015. The water-induced linear reduction gas diffusivity model extended to three pore regions. Vadose Zone J. 14, 1–9. https://doi.org/10.2136/vzj2015.04.0051.

Chirol, C., D. Derrien, L. Saint-André, P. Redon and G. Séré, 2025. Territorial mapping of soil type and land cover influence on ecosystem services. Geoderma Regional. 43, . https://doi.org/10.1016/j.geodrs.2025.e01008.

Currie, J.A. 1960. Gaseous diffusion in porous media. Part 2 - Dry granular materials. British Journal of Applied Physics. 11, 318–324. https://doi.org/10.1088/0508-3443/11/8/303.

da Silva, A.P., B.D. Kay and E. Perfect, 1994. Characterization of the Least Limiting Water Range of Soils. Soil Science Society of America Journal. 58, 1775–1781. https://doi.org/10.2136/sssaj1994.03615995005800060028x.

Danielsen, A.S., C. Pesch, C. Hermansen, C.M. Singleton, T.B.N. Jensen, P.H. Nielsen, M.H. Greve, A. Rudra, H. Sanei, P.L. Weber, E. Arthur, S. Gutierrez, P. Møldrup, S. Normand and L.W. de Jonge, 2025. Soil structure and pH shape prokaryotic communities in lowland soils across Denmark. Geoderma Regional. 43, . https://doi.org/10.1016/j.geodrs.2025.e01016.

Dexter, A.R., G. Richard, D. Arrouays, E.A. Czyż, C. Jolivet and O. Duval, 2008. Complexed organic matter controls soil physical properties. Geoderma. 144, 620–627. https://doi.org/10.1016/j.geoderma.2008.01.022.

Evangelista, S.J., D.J. Field, A.B. McBratney, B. Minasny, W. Ng, J. Padarian, M. Román Dobarco and A.M.J.-. Wadoux, 2024. Chapter One - Soil security—Strategizing a sustainable future for soil. Adv. Agron. 183, 1–70. https://doi.org/10.1016/bs.agron.2023.10.001.

Flint, A.L. and L.E. Flint. 2002. Particle density, in: Methods of soil analysis: Part 4 physical methods. Soil Science Society of America, Madison, WI, USA, pp. 229–240.

Francos, N., A.B. McBratney, D.J. Field, B. Minasny, J.C. Pachon, J. Padarian, A. Hunakunti, W. Ng, S.J. Evangelista and T. O'Donoghue, 2024. Valuing and integrating soil roles in assessing the capital dimension of soil security: An Australian case study. Soil Security. 16, 100141. https://doi.org/10.1016/j.soisec.2024.100141.

Friedlingstein, P., M.W. Jones, M. O'Sullivan, R.M. Andrew, D.C.E. Bakker, J. Hauck, C. Le Quéré, G.P. Peters, W. Peters, J. Pongratz, S. Sitch, J.G. Canadell, P. Ciais, R.B. Jackson, S.R. Alin, P. Anthoni, N.R. Bates, M. Becker, N. Bellouin, L. Bopp, T.T.T. Chau, F. Chevallier, L.P. Chini, M. Cronin, K.I. Currie, B. Decharme, L.M. Djeutchouang, X. Dou, W. Evans, R.A. Feely, L. Feng, T. Gasser, D. Gilfillan, T. Gkritzalis, G. Grassi, L. Gregor, N. Gruber, Ö Gürses, I. Harris, R.A. Houghton, G.C. Hurtt, Y. Iida, T. Ilyina, I.T. Luijkx, A. Jain, S.D. Jones, E. Kato, D. Kennedy, K.K. Goldewijk, J. Knauer, J.I. Korsbakken, A. Körtzinger, P. Landschützer, S.K. Lauvset, N. Lefèvre, S. Lienert, J. Liu, G. Marland, P.C. McGuire, J.R. Melton, D.R. Munro, J.E.M.S. Nabel, S.I. Nakaoka, Y. Niwa, T. Ono, D.

Pierrot, B. Poulter, G. Rehder, L. Resplandy, E. Robertson, C. Rödenbeck, T.M. Rosan, J.ö Schwinger, C. Schwingshackl, R. Séférian, A.J. Sutton, C. Sweeney, T. Tanhua, P.P. Tans, H. Tian, B. Tilbrook, F. Tubiello, G.R. Van Der Werf, N. Vuichard, C. Wada, R. Wanninkhof, A.J. Watson, D. Willis, A.J. Wiltshire, W. Yuan, C. Yue, X. Yue, S. Zaehle and J. Zeng, 2022. Global Carbon Budget 2021. Earth Syst Sci Data. 14, 1917–2005. https://doi.org/10.5194/essd-14-1917-2022.

Hamamoto, S., S.H. Dissanayaka, K. Kawamoto, O. Nagata, T. Komtatsu and P. Moldrup, 2016. Transport properties and pore-network structure in variably-saturated Sphagnum peat soil. Eur. J. Soil Sci. 67, 121–131. https://doi.org/10.1111/ejss.12312.

Hyndman, R.J. and A.B. Koehler, 2006. Another look at measures of forecast accuracy. Int J Forecasting. 22, 679–688. https://doi.org/10.1016/j.ijforecast.2006.03.001.

Iiyama, I., K. Osawa and O. Nagata, 2012. Soil O2 profile affected by gas diffusivity and water retention in a drained peat layer. Soils and Foundations. 52, 49–58. https://doi.org/10.1016/j.sandf.2012.01.005.

Kirschke, S., P. Bousquet, P. Ciais, M. Saunois, J.G. Canadell, E.J. Dlugokencky, P. Bergamaschi, D. Bergmann, D.R. Blake, L. Bruhwiler, P. Cameron-Smith, S. Castaldi, F. Chevallier, L. Feng, A. Fraser, M. Heimann, E.L. Hodson, S. Houweling, B. Josse, P.J. Fraser, P.B. Krummel, J. Lamarque, R.L. Langenfelds, C.L. Quér, V. Naik, S. O'Doherty, P.I. Palmer, I. Pison, D. Plummer, B. Poulter, R.G. Prinn, M. Rigby, B. Ringeval, M. Schmidt, D.T. Shindell, I.J. Simpson, R. Spahni, L.P. Steele, S.A. Strode, K. Sudo, S. Szopa, G.R.v.d. Werf, A. Voulgarakis, M.v. Weele, R.F. Weiss, J.E. Williams and G. Zeng, 2013. Three Decades of

Global Methane Sources and Sinks. Nature Geosci. 6, 813–823. https://doi.org/10.1038/ngeo1955.

Kiuru, P., M. Palviainen, A. Marchionne, T. Grönholm, M. Raivonen, L. Kohl and A. Laurén, 2022. Pore network modeling as a new tool for determining gas diffusivity in peat. BIOGEOSCIENCES. 19, 5041–5058. https://doi.org/10.5194/bg-19-5041-2022.

Kruse, C.W., P. Moldrup and N. Iversen, 1996. Modeling diffusion and reaction in soils II. Atmospheric methane diffusion and consumption in a forest soil. Soil Sci. 161, 355–365. https://doi.org/10.1097/00010694-199606000-00002.

Laurén, A. and H. Mannerkoski, 2001. Hydraulic properties of mor layers in Finland. Scand J Forest Res. 16, 429–441. https://doi.org/10.1080/02827580152632829.

Laurén, A., H. Mannerkoski and T. Orjasniemi, 2000. Thermal and Aeration Properties of Mor Layers in Finland. Scand J Forest Res. 15, 433–444. https://doi.org/10.1080/028275800750172655.

Leifeld, J., C. Wüst-Galley and S. Page, 2019. Intact and managed peatland soils as a source and sink of GHGs from 1850 to 2100. Nat. Clim. Chang. 9, 945–947. https://doi.org/10.1038/s41558-019-0615-5.

Maier, M. and V. Lang, 2019. Gas Diffusivity in the Forest Humus Layer. Soil Sci. 184, 13–16. https://doi.org/10.1097/SS.0000000000000245.

Mikštas, D., L.W. de Jonge, P.L. Weber, A.S. Danielsen, L.W. Kristensen, E. Arthur, P. Møldrup, L. Elsgaard, M.H. Greve and C. Pesch, Drivers of basal respiration rates in intact samples from carbon-rich lowland soils across Denmark. Soil Security.

Millington, R.J. and J.P. Quirk, 1961. Permeability of porous solids. Transactions of the Faraday Society. 57, 1200–1207. https://doi.org/10.1039/TF9615701200.

Moldrup, P., T. Olesen, T. Yamaguchi, P. Schjønning and D.E. Rolston, 1999. Modeling diffusion and reaction in soils. IX. The Buckingham-Burdine-Campbell equation for gas diffusivity in undisturbed soil. Soil Sci. 164, 542–551. https://doi.org/10.1097/00010694-199908000-00002.

Moldrup, P., T. Olesen, J. Gamst, P. Schjønning, T. Yamaguchi and D.E. Rolston, 2000. Predicting the Gas Diffusion Coefficient in Repacked Soil Water-Induced Linear Reduction Model. Soil Sci. Soc. Am. J. 64, 1588–1594. https://doi.org/10.2136/sssaj2000.6451588x.

Moldrup, P., T. Olesen, P. Schjønning, T. Yamaguchi and D.E. Rolston, 2000. Predicting the Gas Diffusion Coefficient in Undisturbed Soil from Soil Water Characteristics. Soil Sci. Soc. Am. J. 64, 94–100. https://doi.org/10.2136/sssaj2000.64194x.

Moldrup, P., T. Olesen, T. Komatsu, P. Schjønning and D.E. Rolston, 2001. Tortuosity, Diffusivity, and Permeability in the Soil Liquid and Gaseous Phases. Soil Sci. Soc. Am. J. 65, 613–623. https://doi.org/10.2136/sssaj2001.653613x.

Moldrup, P., T. Olesen, S. Yoshikawa, T. Komatsu and D.E. Rolston, 2004. Three-Porosity Model for Predicting the Gas Diffusion Coefficient in Undisturbed Soil. Soil Sci. Soc. Am. J. 68, 750–759. https://doi.org/10.2136/sssaj2004.7500.

Moldrup, P., T. Olesen, H. Blendstrup, T. Komatsu, L.W. de Jonge and D.E. Rolston, 2007. Predictive-descriptive models for gas and solute diffusion coefficients in variably saturated porous media coupled to pore-size distribution: IV. Solute diffusivity and the liquid phase impedance factor. Soil Sci. 172, 741–750. https://doi.org/10.1097/SS.0b013e3180d0a423.

Moldrup, P., T.K. Chamindu Deepagoda K., S. Hamamoto, T. Komatsu, K. Kawamoto, D.E. Rolston and L.W. de Jonge, 2013. Structure-dependent water-induced linear reduction model for predicting gas diffusivity and tortuosity in repacked and intact soil. Vadose Zone J. 12, 1–11. https://doi.org/10.2136/vzj2013.01.0026.

Nash, J.E. and J.V. Sutcliffe, 1970. River flow forecasting through conceptual models part I — A discussion of principles. J. Hydrol. (Amst.). 10, 282–290. https://doi.org/10.1016/0022-1694(70)90255-6.

Nielsen, J.E., D. Karup, J. Lis W De, M. Ahm, T.R. Bentzen, M.R. Rasmussen and P. Moldrup, 2018. Can the volume ratio of coarse to fine particles explain the hydraulic properties of sandy soil? 82, 1093–1100. https://doi.org/10.2136/sssaj2018.02.0083.

Page, S.E., J.O.&. Rieley and C.J. Banks, 2011. Global and regional importance of the tropical peatland carbon pool. Global Change Biol. 17, 798–818. https://doi.org/10.1111/j.1365-2486.2010.02279.x.

Penman, H.L. 1940. Gas and vapor movements in soil: The diffusion of vapors through porous solids. The Journal of Agricultural Science. 30, 437–462. https://doi.org/10.1017/S0021859600048164.

Pesch, C., P.L. Weber, L.W. de Jonge, M.H. Greve, T. Norgaard and P. Moldrup, 2021. Soil–air phase characteristics: Response to texture, density, and land use in Greenland and Denmark. Soil Science Society of America Journal. 85, 1534–1554. https://doi.org/10.1002/saj2.20284.

Petersen, L.W., D.E. Rolston, P. Moldrup and T. Yamaguchi, 1994. Volatile Organic Vapor Diffusion and Adsorption in Soils. Journal of Environmental Quality. 23, 799–805. https://doi.org/10.2134%2Fjeq1994.00472425002300040026x.

Pittaki-Chrysodonta, Z., P. Moldrup, M. Knadel, B.V. Iversen, C. Hermansen, M.H. Greve and L.W. de Jonge, 2018. Predicting the Campbell soil water retention function: Comparing visible–near-infrared spectroscopy with classical pedotransfer function. Vadose Zone Journal.170169. https://doi.org/10.2136/vzj2017.09.0169.

Pozza, L.E. and D.J. Field, 2020. The science of Soil Security and Food Security. Soil Security. 1, 100002. https://doi.org/10.1016/j.soisec.2020.100002.

Rezanezhad, F., J.S. Price and J.R. Craig, 2012. The effects of dual porosity on transport and retardation in peat: A laboratory experiment. Can. J. Soil Sci. 92, 723–732. https://doi.org/10.4141/CJSS2011-050.

Rolston, D.E. and P. Moldrup. 2012. Gas transport in soil, in: Huang, P.M., Li, Y., Sumner, M.E. (ed.) Handbook of soil science: Properties and processes. CRC Press, , pp. 1–20.

Rolston, D.E. and P. Moldrup. 2002. Gas diffusivity, in: G. Clarke Topp and J.H. Dane (eds.) Methods of soil analysis: Part 4 physical methods. Soil Science Society of America, Madison, WI, USA, pp. 1113–1139.

Ruehlmann, J. 2020. Soil particle density as affected by soil texture and soil organic matter: 1. Partitioning of SOM in conceptional fractions and derivation of a variable SOC to SOM conversion factor. Geoderma. 375, 114542. https://doi.org/10.1016/j.geoderma.2020.114542.

Rust, R.H., A. Klute and J.E. Gieseking, 1957. Diffusion-Porosity Measurements using a nonsteady state system. Soil Science. 84, 453–464.

Saunois, M., A.R. Stavert, B. Poulter, P. Bousquet, J.G. Canadell, R.B. Jackson, P.A. Raymond, E.J. Dlugokencky, S. Houweling, P.K. Patra, P. Ciais, V.K. Arora, D. Bastviken, P. Bergamaschi, D.R. Blake, G. Brailsford, L. Bruhwiler, K.M. Carlson, M. Carroll, S. Castaldi, N. Chandra, C. Crevoisier, P.M. Crill, C.L. Curry, G. Etiope, C. Frankenberg, N. Gedney, M.I. Hegglin, L. Höglund-Isaksson, G. Hugelius, M. Ishizawa, A. Ito, G. Janssens-Maenhout, K.M. Jensen, F. Joos, T. Kleinen, P.B. Krummel, R.L. Langenfelds, G.G. Laruelle, L. Liu, T. Machida, S. Maksyutov, K.C. McDonald, J. McNorton, P.A. Miller, J.R. Melton, I. Morino, J. Müller, F. Murguia-Flores, V. Naik, Y. Niwa, S. Noce, S. O'Doherty, R.J. Parker, C. Peng, S. Peng, G.P. Peters, C. Prigent, R. Prinn, M. Ramonet, P. Regnier, W.J. Riley, J.A. Rosentreter, A. Segers, I.J. Simpson, H. Shi, S.J. Smith, L.P. Steele, B.F. Thornton, H. Tian, Y. Tohjima, F.N. Tubiello, A. Tsuruta, N. Viovy, A. Voulgarakis, T.S. Weber, M.v. Weele, G.R.v.d. Werf, R.F. Weiss, D. Worthy, D. Wunch, Y. Yin, Y. Yoshida, W. Zhang, Z. Zhang, Y. Zhao, B. Zheng, Q. Zhu, Q. Zhu and Q. Zhuang, 2020. The Global Methane Budget 2000–2017. Earth Syst Sci Data. 12, 1561–1623. https://doi.org/10.5194/essd-12-1561-2020.

Schjønning, P. 1992. Size distribution of dispersed and aggregated particles and of soil pores in 12 Danish soils. Acta Agr Scand B-s P. 42, 26–33. https://doi.org/10.1080/09064719209410196.

Schjønning, P., L.J. Munkholm, S. Elmholt and J.E. Olesen, 2007. Organic matter and soil tilth in arable farming: Management makes a difference within 5–6 years. Agr Ecosyst Environ. 122, 157–172. https://doi.org/10.1016/j.agee.2006.12.029.

Schjønning, P., M. Eden, P. Moldrup and L.W. de Jonge, 2013. Two-Chamber, Two-Gas and One-Chamber, One-Gas Methods for Measuring the Soil-Gas Diffusion Coefficient: Validation and Inter-calibration. Soil Science Society of America Journal. 77, 729–740. https://doi.org/10.2136%2Fsssaj2012.0379.

Weber, P.L., L.W. de Jonge, M.H. Greve, T. Norgaard and P. Moldrup, 2020. Gas diffusion characteristics of agricultural soils from South Greenland. Soil Sci. Soc. Am. J. 84, 1606–1619. https://doi.org/10.1002/saj2.20114.

Yin, K., A. Fauchille, E. Di Filippo, P. Kotronis and G. Sciarra, 2021. A Review of Sand–Clay Mixture and Soil–Structure Interface Direct Shear Test. Geotechnics (Basel). 1, 260–306. https://doi.org/10.3390/geotechnics1020014.

Zhu, D., P. Ciais, G. Krinner, F. Maignan, A. Jornet Puig and G. Hugelius, 2019. Controls of soil organic matter on soil thermal dynamics in the northern high latitudes. Nat Commun. 10, 3172–9. https://doi.org/10.1038/s41467-019-11103-1.

Table 1: Table overview of relevant soil parameters included in this study; Soil organic carbon content (SOC), bulk density (BD), particle density (PD), total porosity (Φ), air-filled porosity at pF3 (ε*), Campbell b and Buckingham X

SOC interval [%]	**Locations (N)**	**SOC [%]**	**BD [g/cm^3]**	**PD [g/cm^3]**	**Φ [cm^3/cm^3]**	**ε* [cm^3/cm^3]**	**Campbell b**	**Buckingham X**
12-18%	22	15.13	0.72	2.28	0.72	0.30	9.24	2.27
18-24%	21	20.71	0.49	2.16	0.77	0.34	8.90	2.48
24-30%	20	26.99	0.47	2.02	0.77	0.29	10.95	2.43
30-36%	29	33.13	0.38	1.92	0.81	0.34	9.44	2.79
36-42%	14	39.46	0.32	1.79	0.82	0.33	9.20	2.35
>42 %	21	45.96	0.28	1.69	0.83	0.35	8.41	2.86
Total	127							
Range		12.56-52.06	0.09-1.19	1.54-2.57	0.51-0.95	0.10-0.68	3.47-23.75	
Average		29.81	0.43	1.99	0.79	0.33	9.37	2.53

Table 2: overview of model performance for the selected D_p/D_0 models. RMSE: Root Mean Square Error; NSE: Nash-Sutcliffe model efficiency coefficient and AIC: Akaike's Information Criterion.

Reference	Model name	Eq. no.	Equation	RMSE	NSE	AIC	No. of variables (AIC)
Buckingham (1904)	Buckingham – original	[2]	$\frac{D_p}{D_0} = \varepsilon^2$	0.042	-0.287	-2660	1
Weber et al. (2020)	Weber model	[2]	$\frac{D_p}{D_0} = \varepsilon^{2.50}$	0.026	0.516	-3404	1
Penman (1940)	Penman 1940	[3]	$\frac{D_p}{D_0} = 0.66\varepsilon$	0.114	-8.499	-1139	1
Millington and Quirk (1961)	Millington and Quirk	[4]	$\frac{D_p}{D_0} = \frac{\varepsilon^{\frac{10}{3}}}{\Phi^2}$	0.029	0.388	-3224	2
Moldrup et al. (2000a)	WLR Marshall	[5]	$\frac{D_p}{D_0} = 0.66\varepsilon\frac{\varepsilon}{\Phi}$	0.027	0.442	-3295	2
Moldrup et al. (2000b)	Macro-porosity dependent model	[6]	$\frac{D_p}{D_0} = 2\varepsilon^3 + 0.04\varepsilon$	0.047	-0.596	-2496	1
Chamindu et al. (2011)	Generalized Density-Corrected Model (GDC)	[7]	$\frac{D_p}{D_0} = 0.5\Phi(\frac{\varepsilon}{\Phi})^{2+1.38\Phi}$	0.036	0.086	-2918	2
Moldrup et al. (1999)	Buckingham-Burdine-Campbell model	[8]	$\frac{D_p}{D_0} = \Phi^2(\frac{\varepsilon}{\Phi})^{2+3b}$	0.022	0.655	-3606	3
This study	Effective porosity modifed WLR model	[9]	$\frac{D_p}{D_0} = 0.25\varepsilon\frac{\varepsilon}{\varepsilon^*}$	**0.015**	**0.847**	**-4280**	**2**

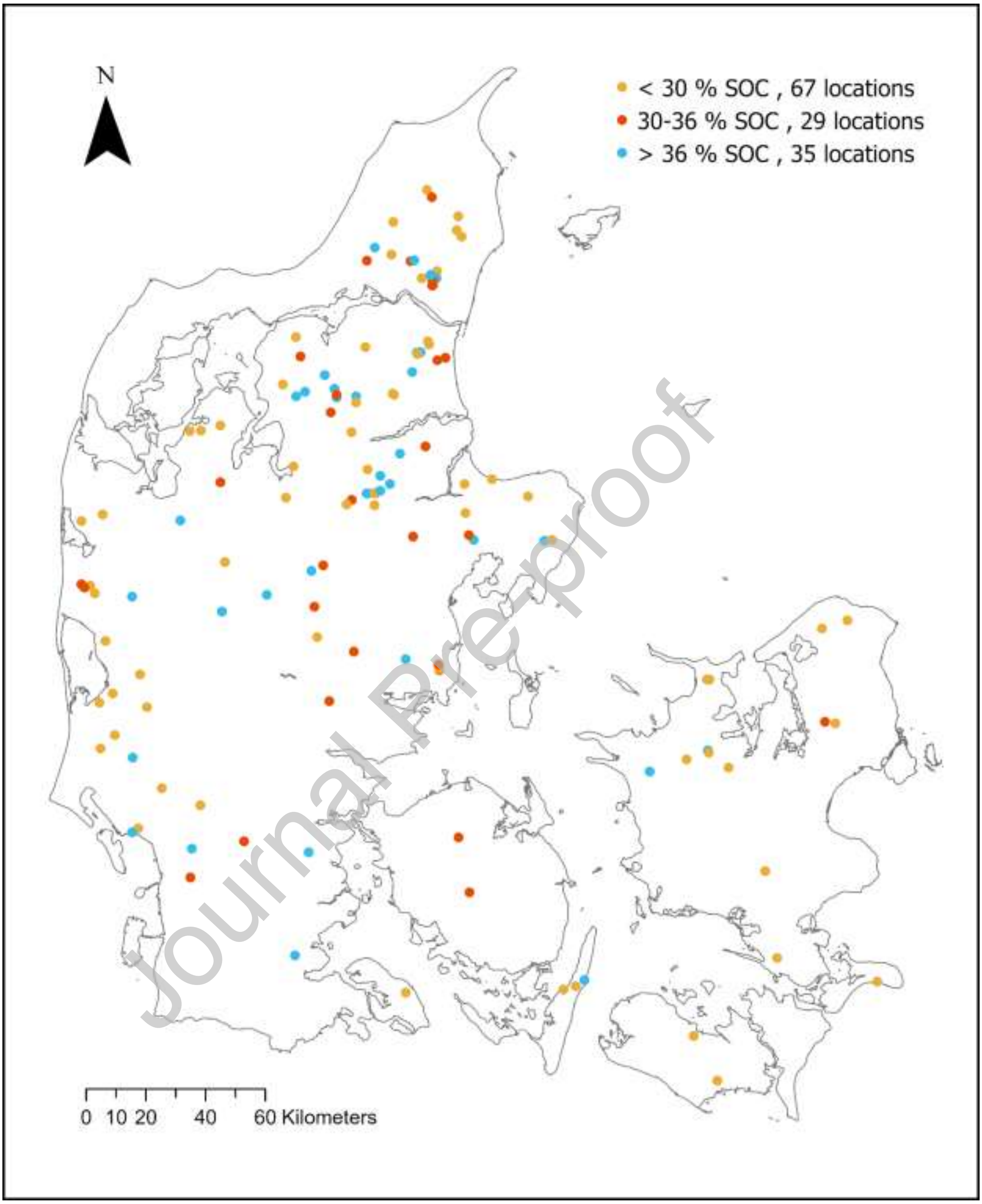

Figure 1. Map of the investigated 127 peat soil locations across Denmark. The three different colors represent three ranges of soil organic carbon (SOC) content: <30 % SOC (yellow), N=67), 30-36% SOC (red, N=29), and >36% SOC (blue, N=35)

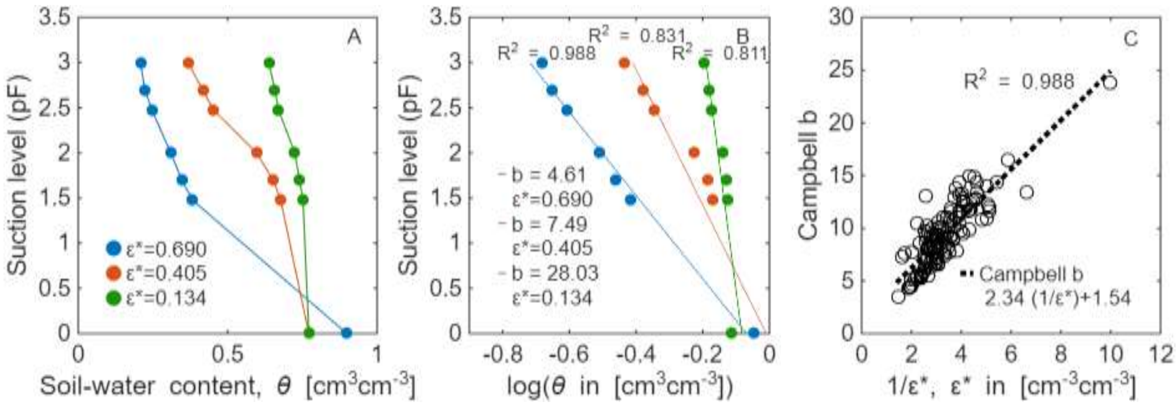

Figure 2. Examples of variations in soil-water characteristics, (A) Soil-water retention curves for three peat soil samples with almost identical soil organic carbon (SOC) content at 34.63% (green), 35.03% (blue), and 35.62% (orange). The effective porosity (ε*) is the difference between total porosity and water content at pF 3. (B) Linearized water retention curves and determination of the Campbell (1974) pore-size distribution index (Campbell b), and (C) the relation between Campbell b and inverse of the effective porosity e* for all peat soil samples.

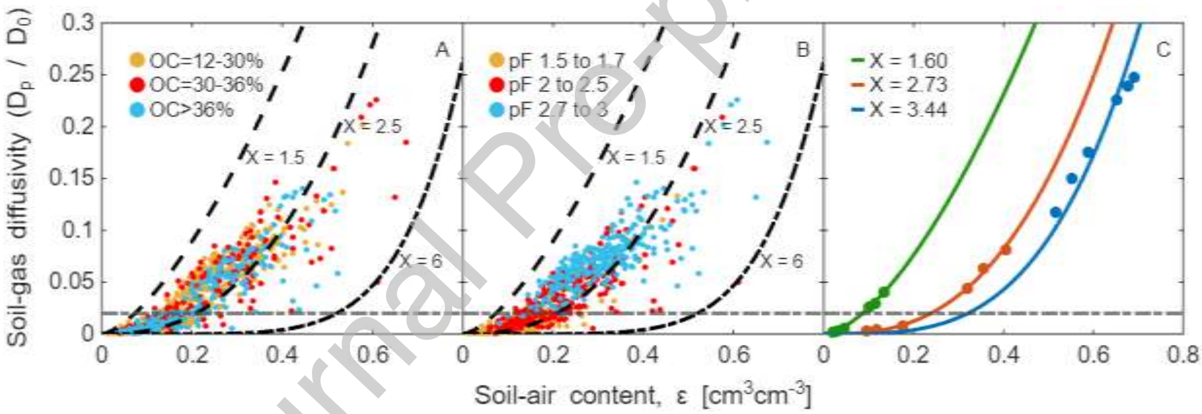

Figure 3. Overview of soil-gas diffusivity (D_p/D_0) data. (A) D_p/D_0 versus soil-air content (ε) for the three different SOC classes as shown in Fig. 1, (B) D_p/D_0 versus ε for three different soil moisture levels (wet: pF 1.5-1.7; moist: pF 2-2.5; and dry: pF 2.7-3), and (c) gas diffusivity curves ($D_p/D_0 = \varepsilon^X$ with X fitted to the measured data) for the same three soil samples shown in Fig. 2A-B (SOC = 34.63% (green), 35.03% (blue) and 35.62% (orange)). Also shown is the often-considered limit for adequate soil aeration, $D_p/D_0 = 0.02$ (Schjønning et al., 2007), upper and lower limits of the Buckingham tortuosity-connectivity index (X = 1.5 and X=6.0, respectively), and the Weber et al. (2020) model for higher-organic soils (X = 2.5).

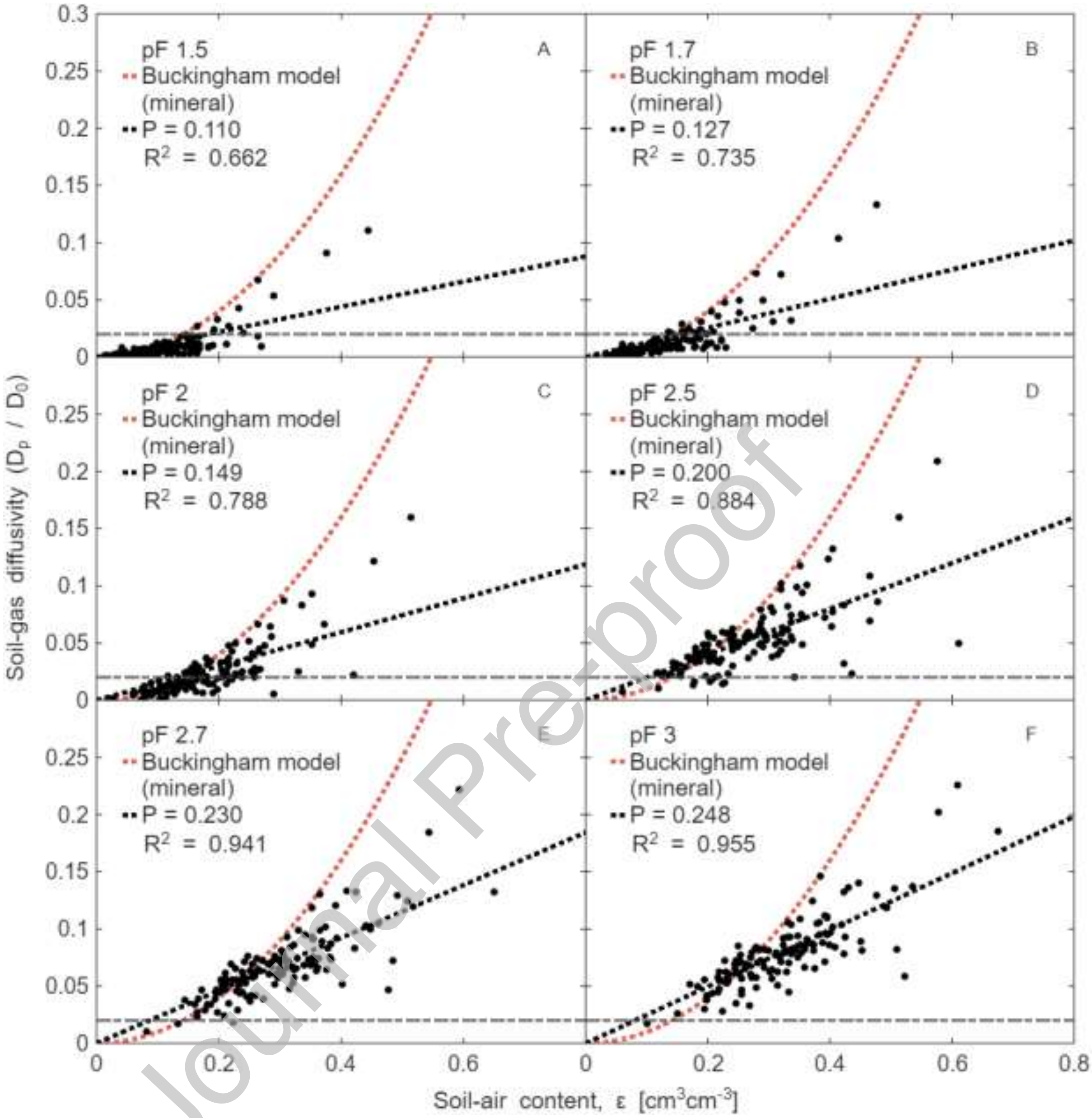

Figure 4. Gas diffusivity (D_p/D_0) versus soil-air content (ε) for each of the six suction (pF) levels. Also shown are the best fit of the Penman (1940) gas diffusivity model (dotted black line) and the best-fit values of the Penman pore continuity index (P) increasing with increasing pF values (from A to F). Additionally, the Buckingham (1904) gas diffusivity model (red dotted line) is normally representative for mineral (low-organic) soils.

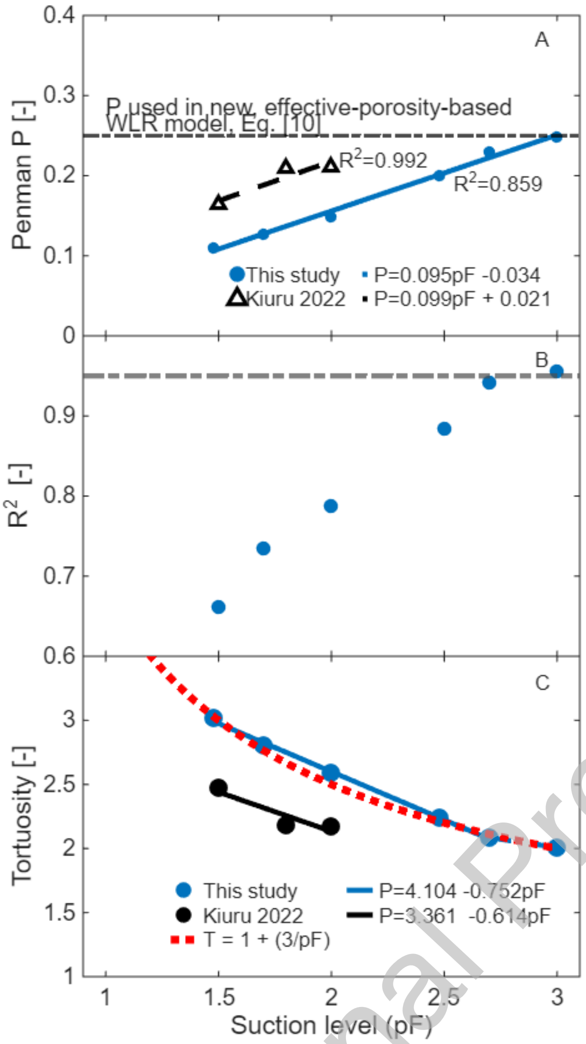

Figure 5. (A) Penman pore continuity index (P) as a function of pF, following analyses in Fig. 4A-F, (B) R^2 of linear fit between D_p/D_0 and ε for the Penman model with different indices. Here shown as a function of pF, and (C) derived pore-network tortuosity, $T = \sqrt{\frac{\varepsilon}{\frac{D_p}{D_0}}} = \sqrt{\frac{1}{P}}$ as a function of pF.

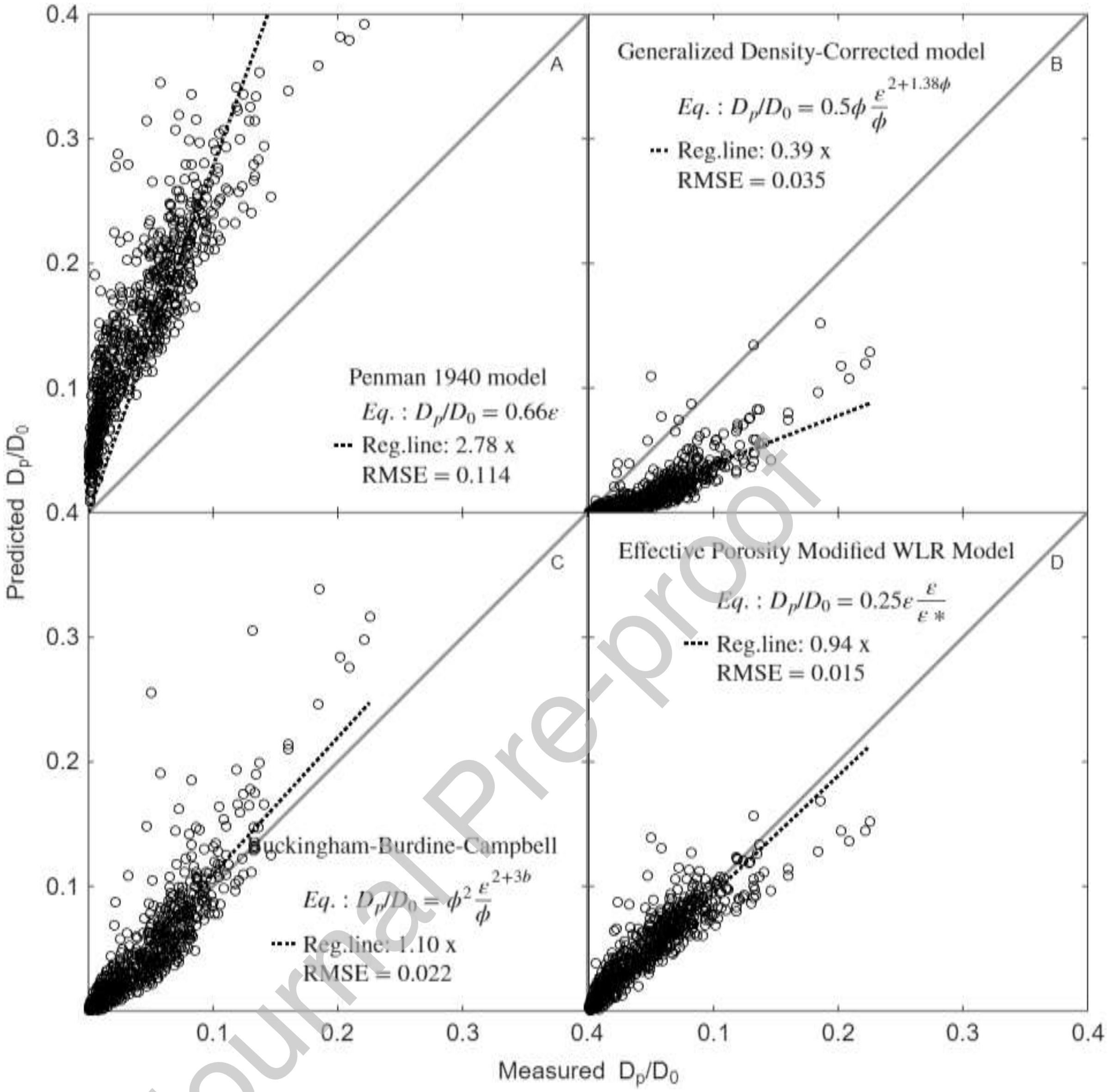

Figure 6. Scatter-plot performance of four selected gas diffusivity (D_p/D_0) models: (A) Penman (1940) that is still frequently used across scales for evaluation of C and N dynamics in both normal and peat land soils, (B) the also frequently used Generalized Density Corrected (GDC) model developed for mineral (low-organic) soils, (c) the Buckingham-Burdine-Campbell (BBC) soil-water characteristic dependent model, and (D) the new ε*-modified Water-induced Linear Reduction (WLR) model. For further model tests and an overview of model performance statistics for the 127 peat soils, see Table 2.

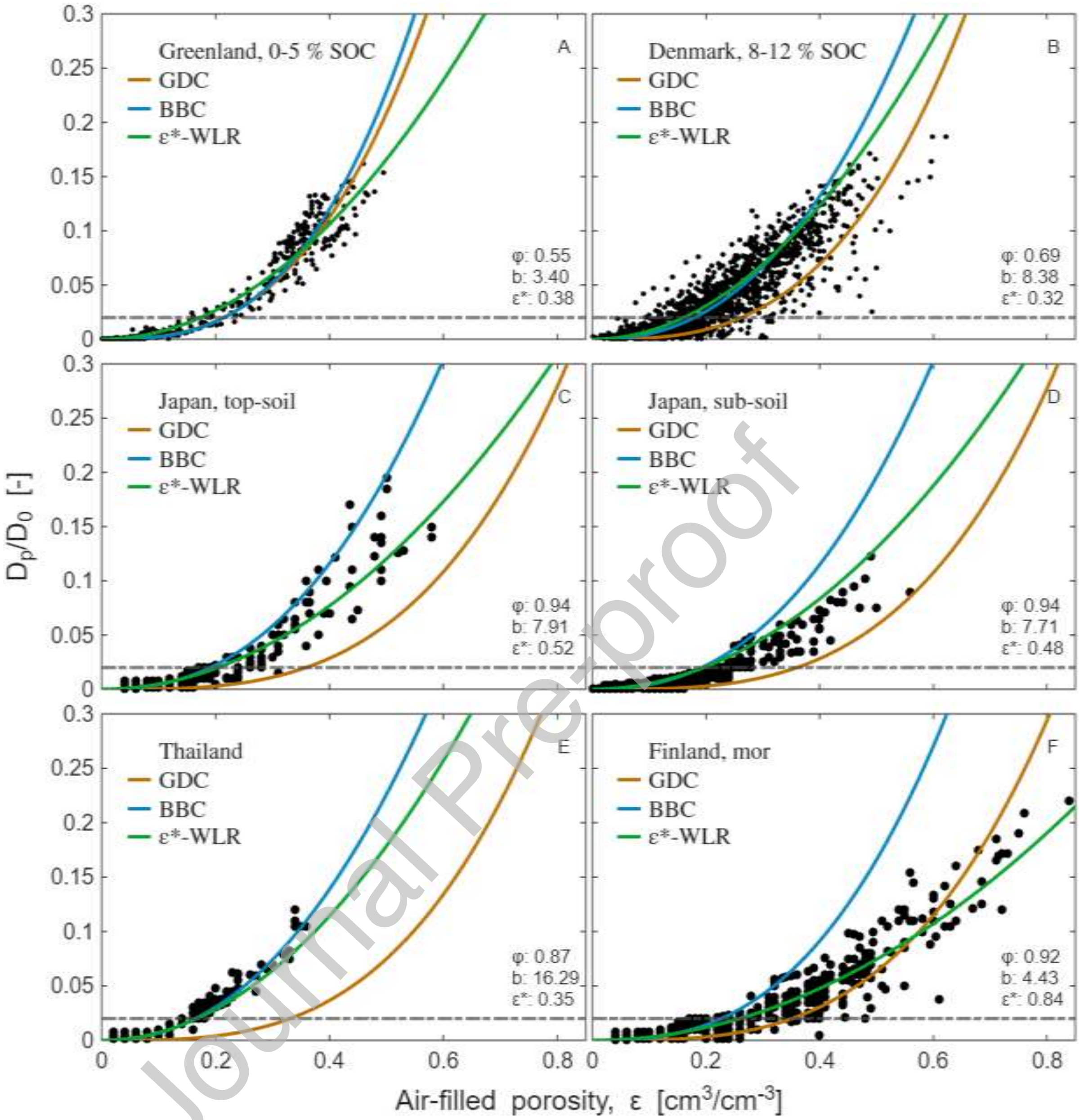

Figure 7. Gas diffusivity (D_p/D_0) versus soil-air content (ε) for different soils from across the world. Independent model test of the ε* modified WLR model (green), GDC (orange) and BBC (blue) models. The models were compared to (A) Greenlandic mineral-dominated (0-5 % SOC) soils (Pesch et al., 2021), (B) Danish lowland non-peat soils (present study), (C) and (D) Japanese top and sub- peat soils at decomposed condition (C) and at pristine peat condition (D) (Iiyama et al., 2012), (E) Thai oil palm field (Iiyama et al., 2012), and (F) Finnish mor soils (Laurén and Mannerkoski, 2001; Laurén et al., 2000).

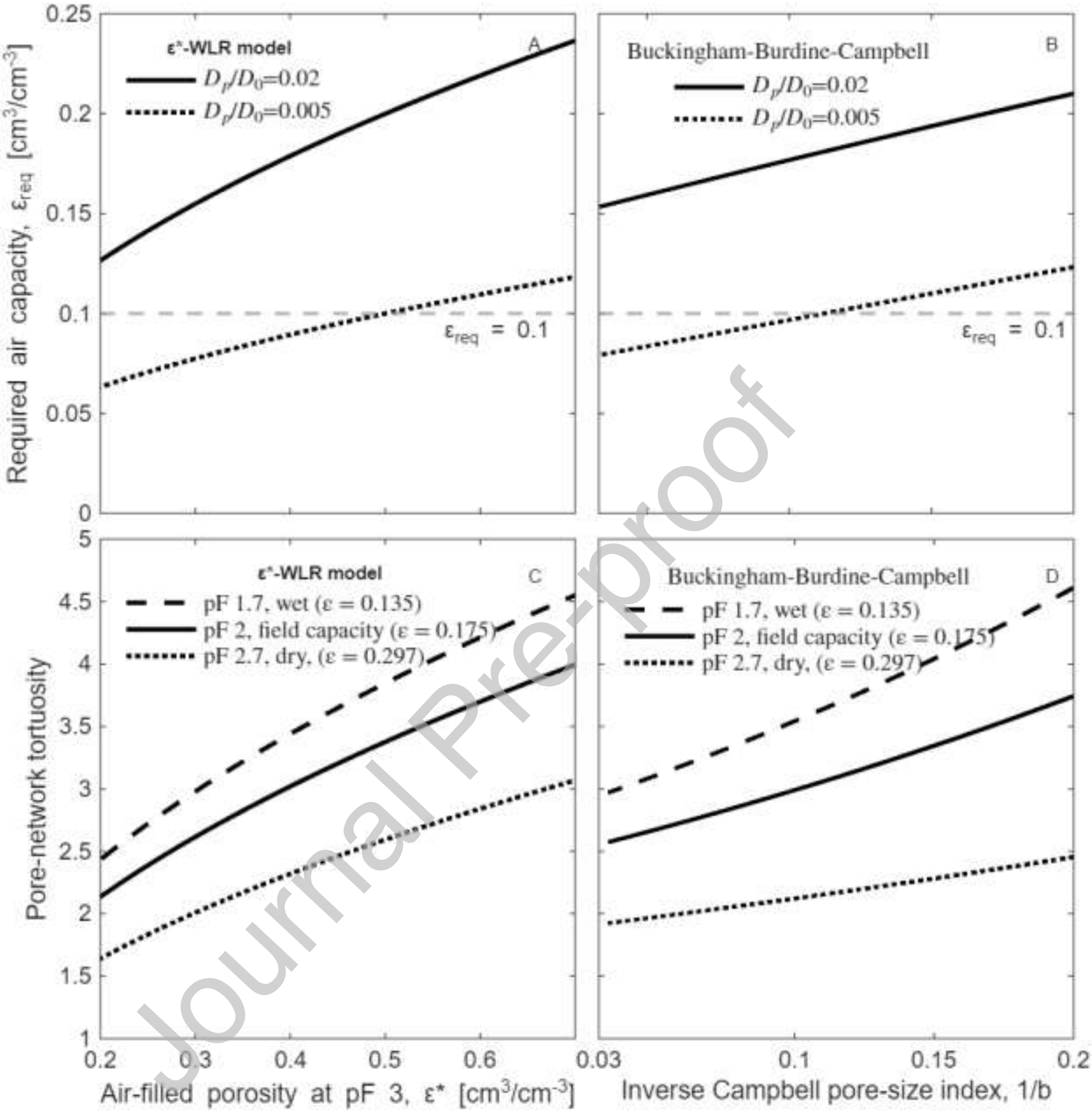

Figure 8. The required air-filled porosity to reach limited gas transport (D_p/D_0 = 0.005) and full soil aeration (D_p/D_0 = 0.02) as a function of (A) air-filled porosity at pF 3 (ε*) in the ε*-modified WLR model, and (B) the inverse Campbell pore-size distribution index, b, in the BBC model. Also shown is the air-filled porosity traditionally considered as adequate for full soil aeration (0.1 cm^3/cm^3; grey dotted line). (C) and (D) Pore-network tortuosity, T, as a function of (C) air-filled porosity at pF 3 and (D) inverse Campbell pore-size distribution index, b. For remaining input to the ε* modified WLR and BBC models, average parameter values were used (Table 1).

GRAPHICAL ABSTRACT

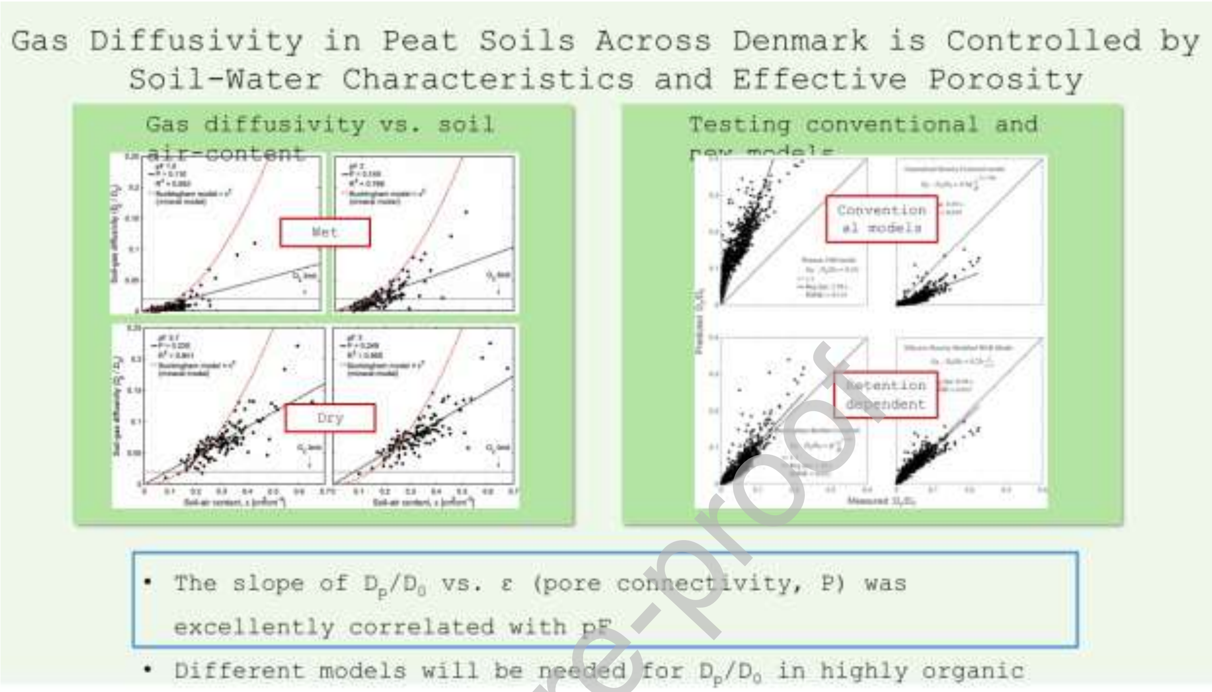

Declaration of interests

☒ The authors declare that they have no known competing financial interests or personal relationships that could have appeared to influence the work reported in this paper.